Adsorptive removal of hazardous azorhodanine dye from an aqueous solution using rice straw fly ash

A.A. El-Bindary*, A.Z. El-Sonbati, A.F. Shoair, A.S. Mohamed

Department of Chemistry, Faculty of Science, University of Damietta, Damietta 34517, Egypt.

*Corresponding author. Tel.: +2 0114266996; Fax: +2 0572403868
E-mail address: abindary@yahoo.com (A.A. El-Bindary).

Abstract

The objective of this study was to assess the suitability and efficiency of rice straw fly ash (RSFA) for the removal of hazardous azorhodanine dye (AR) from aqueous solution. The effect of different variables in the batch method as a function of solution pH, contact time, concentration of adsorbate, adsorbent dosage and temperature were investigated and optimal experimental conditions were ascertain. More than 85 % removal efficiency was obtained within 75 min. at adsorbent dose of 0.07 g for initial dye concentration of 20-100 mg/L at pH 3.The experimental equilibrium data were tested by the isotherm models namely, Langmuir and Freundlich adsorption and the isotherm constants were determined. The kinetic data obtained with different initial concentration and temperature wasanalyzed using a pseudo-first-order and pseudo-second-order equations. The activation energy of adsorption was also evaluated and found to be +11.09 kJ.mol^{-1}indicating that the adsorption is physisorption.Various thermodynamic parameters, such as Gibbs free energy, entropy and enthalpy of the on going adsorption process have been calculated and found to be spontaneous and exothermic, respectively. The results indicate that (RSFA) could be employed as low-cost material for the removal of acid dyes from aqueous solution.

Keywords: Adsorption; Rice straw fly ash; Water treatment; Thermodynamics.

1. Introduction

Water contamination caused by dye industries, including food, leather, textile, plastic, cosmetics, paper-making, printing and dye synthesis, has caused more and more attention, since most dyes are harmful to human being and environments [1]. Therefore, these industrial effluents must be treated before discharge. Currently, much attention has been paid to the removal of dyes from industrial wastewater [2]. Various treatment methods including physical, chemical and biological schemes have been developed to remove dyes from wastewater [3]. However, these methods mentioned above always show some disadvantages, such as the generation of large amounts of toxic and carcinogenic by products, energy intensive and high cost. Some of the applied techniques for the treatment of dye contaminated wastewaters are flocculation, coagulation, precipitation, adsorption, membrane filtration, electrochemical techniques, ozonation and fungal decolorization [4,5]. Among them, the adsorption based procedure widely utilized due to its high efficiency, capacity and ability for large scale dye removal application (with potential for adsorbent regeneration) [6-9]. The nontoxic, low cost and easy availability adsorbents are the best choice for wastewater treatment. Due to the unique properties of nanoparticles such as a high number of reactive atoms, high mechanical and thermal strength, large number of vacant reactive surface sites metallic or semi-metallic behavior and high surface area widely applied for removal of various toxic materials [10]. Activated carbon as one of the most common building blocks of nanotechnology is the low cost and general material as support for loading nanomaterial [11]. To our delight, adsorption is an economic, effective and easily operated process in dye removal [12]. Numerous adsorbents, such as zeolite, silica, wheat shells, orange peel, coir pith, almond shells, natural polymeric materials, etc. have been studied and applied [13].

The industrial wastewater usually contains a variety of organic compounds and toxic pulp mills and dyestuff manufacturing discharge highly coloredwastewater which has provoked serious environmental concerns all over the world [14]. Several methods including adsorption [15], coagulation [16], membrane filtration [17] and advanced oxidation [18] have been employed to eliminate dyes from wastewaters. Among them, adsorption has been recognized as a promising technique due to its high efficiency, simplicity of design,

ease of operation as well as the wide suitability for diverse types of dyes [19,20].Because the dye effluent may cause damage to aquatic biota and human by mutagenic and carcinogenic effects, the removal of dye pollutants from wastewater is of great importance [21].

Fly ash is a waste material originating in large quantities from modern power stations. Although it has been successfully used as a mineral admixture in concrete and brick production, there are still superfluous fly ashes in some countries, causing environmental and disposal problem. The utilization of fly ash as adsorbent for dye removal from industrial wastewater could be rewarding to both environment and economy. Thus many efforts were attempted to make fly ash a cheap adsorbent for dye removal in recent years [22,23]. Many works were focused on the absorption property of fly ash, and some treatments were carried out to improve its adsorption capacity, such as sonochemical treatment [24], microwave heating [25] and H_2O_2 treatment [26]. Different fly ashes may be different in their adsorption behaviors, and more efforts should be made to improve their adsorption capabilities. In Egypt, rice straw fly ash is an easily available agricultural waste material, produced in large quantities as a by-product of rice milling and create potential environmental problems. The waste products which are the main contributors to biomass burning are wheat residue and rice straw. The disposal of rice straw by open-field burning frequently causes serious air pollution, hence new economical technologies for rice straw disposal and utilization must be developed.

The aim of this study is to investigate the adsorption of hazardous azorhodanine dye onto rice straw as a waste adsorbent. Effects of different parameters such as initial adsorbate concentration, adsorbent dosage, contact time, solution pH and temperature were studied. The kinetic and thermodynamic parameters were also calculated to determine rate constants and adsorption mechanism. The experimental data were fitted into Langmuir and Freundlich equations to determine which isotherm gives the best correlation to experimental data.

2. Materials and methods

2.1. Physical measurements

C, H and N were determined on Automatic Analyzer CHNS Vario ELIII, Germany. Spectroscopic data of the azorhodanine dye were obtained using the following instruments: FT-IR spectra (KBr discs, 4000-400 cm^{-1}) by Jasco-4100 spectrophotometer; the ^{1}H NMR spectrum by Bruker WP 300 MHz using DMSO-d_6 as a solvent containing TMS as the internal standard; Mass spectrum by Shimadzu GC-MS-QP2010 Plus instrument. The SEM results of the ACRS sample before and after the adsorption processes were obtained using (JEOL-JSM-6510 LV) scanning microscope to observe surface modification. UV-visible spectrophotometer (Perkin-Elmer AA800 Model AAS) was employed for absorbance measurements of samples. The pH meter model-MP220 (Mettler-Toledo AG, CH-8603) and a Gallenkamp Orbital Incubator were used for pH adjustment and shaking, respectively. N_2 adsorption/desorption isotherms on ACRS at 77 K was measured on a Quantachrome Nova Instruments version 10, from which the Brunauer-Emmett-Teller (BET) surface area and Barrett-Joyner-Halenda (BJH) pore volume were calculated.

2.2. Synthesis of azorhodaninedye

4-((4-hydroxy-3-(4-sulfamoylphenyl)-2-thioxo-2,3-dihydrothiazol-5-yl)diazenyl) benzenesulfonic acid (Fig.1) was prepared [27] by gradual addition of an aqueous solution of 0.01 mole of sodium nitrite to a concentrated hydrochloric acid solution of 0.01 mole of sulphanilic acid with stirring and kept for about 20 min. in the ice bath.
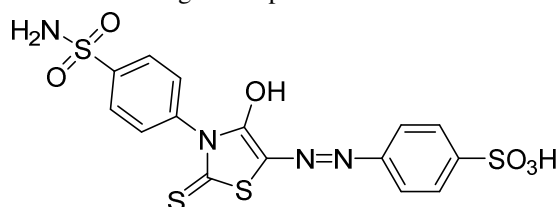

Fig. 1. The structure of azorhodanine dye (AR).

The formed diazonium chloride solutions were added gradually with vigorous stirring to a 0.01 mole cold solution of 3-sulfamoylphenylaminorhodanine in 50 ml pyridine. The reaction mixture was stirred for 2-3 h until coupling was complete. The solid precipitate was filtered, washed with water, dried and crystallized from ethanol and then dried in a vacuum desiccator over anhydrous calcium chloride. Yield 70 %; brown solid; mp = 170 °C; Anal.: Calcd. for $C_{15}H_{12}N_4O_6S_4$ (472.52): C, 38.13; H, 2.56; N, 11.86; 32. Found: C, 38.18; H, 2.61; N, 11.89; 32. FT-IR spectrum IR (KBr) (v cm^{-1}): 3410 (OH), 3345, 3247 (NH$_2$) 1556 (N=N) cm^{-1}. ^{1}H-NMR spectrum in d_6-DMSO, ppm: 7.50-8.0 (m, 10H, Ar-H+NH$_2$), 10.89 (s, 1H, OH).

2.3. Preparation of rice straw fly ash

Rice straw fly ash (RSFA)as adsorbent was collected from Tammy Amdid, Dakahlia, Egypt Biogas Factory [15]. In our laboratory the rice straw fly ash (RSFA) wascrushed, ground and sieved through a 200 µm sieveandwashed several times with bidistilled water. The adsorbent sample was dried at 120°C for 48 h. preserved in the desiccators over anhydrous $CaCl_2$ for further use.FT-IR spectrum of RSFA is of vital importance in understanding the adsorption process and used to determine the vibrational frequencies of RSFA. In RSFA the FT-IR adsorption peaks are: IR (KBr) (v cm^{-1}): 3397 (-SiOH or -OH), 1585 (C=O), 1195 (Si-O-Si) and 792 (Si-H) cm^{-1}[28].

2.4. Adsorption experiments

Batch adsorption studies were carried out by shaking 50 ml conical flasks containing 0.07 g of (RSFA) and 25 mL of dye solutions of desired concentration with adjusted pH on an orbital shaker machine at 200 rpm at 25 °C. The solution pH was adjusted with 0.1 mol/L HCland 0.1 mol/L NaOH solutions. At the end of the adsorption period, the supernatant solution was separated by centrifugation at 200 rpm for 10 min. Then the concentration of the residual dye was determined spectrophotometrically by monitoring the absorbance at 265 nm for dye using UV–Vis spectrophotometer. Percentage of Dye removal (R) was calculated using eq. (1):

$$R = 100 (C_0 - C_t) / C_0 \qquad (1)$$

where C_0 (mg/L) and C_t (mg/L) are dye concentration initially and at time t, respectively. For adsorption isotherms, dye solutions different concentrations (20–100 mg/L) were agitated with known amounts of adsorbents until the equilibrium was achieved. Equilibrium adsorption capacity, q_e (mg dye per g adsorbent) was calculated from the following eq. (2):

$$q_e = V (C_0 - C_t) / W \qquad (2)$$

whereC_t (mg/L) is the dye concentration at equilibrium, V (L) is the volume of solution and W (g) is the weight of adsorbent.

The procedures of kinetic experiments were identical with those of equilibrium tests. At predetermined moments, aqueous samples (5 mL) were taken from the solution, the liquid was separated from the adsorbent by centrifuge at 200 rpm and concentration of Dye in solution was determined spectrophotometrically at a wavelength of 265 nm. The amount of Dye adsorbed at time t, q_t (mg/g) was calculated by following eq. (3):

$$q_t = V (C_0 - C_t) / m \qquad (3)$$

where C_0 (mg/L) is the initial dye concentration, C_t (mg/L) the dye concentration at any time t, V (L) the volume of the solution and m (g) is the mass of the adsorbent [29].

3. Results and discussion

3.1. Brunauer-Emmett-Teller (BET) surface area.

The Brunauer-Emmett-Teller (BET) [30] surface area and Barrett-Joyner-Halenda (BJH) pore size of RSFA have been investigated previously [27] using N_2 adsorption/desorption measurements at 77 K. The BET surface area of RSFA was obtained as 67.4 m^2/g can supply more surface active sites, leading to an enhancement of adsorption performance. It is suggested that the pore structure of the adsorbent ACRS consists of macropores, mesopores and micropores. The total pore volume (V_p) at P/P_o = 0.959 was obtained as 0.134 cm^3/g, which indicating that RSFA has a mesoporous structure and makes it easy for azorhodaninedye to penetrate into the mesopores of RSFA.

3.2. SEM analysis

Scanning electron microscopy (SEM) has been a primary tool for characterizing the surface morphology and fundamental physical properties of the adsorbent surface. It is useful for determining the particle shape, porosity and appropriate size distribution of the adsorbent. It is clear that, raw (RSFA) has considerable numbers of pores where, there is a good possibility for dyes to be trapped and adsorbed into these pores [22]. The SEM picture of (RSFA) adsorbed with tested dye (AR) shows very distinguished dark spots which can be taken as a sign of effective adsorption of azorhodanine molecules in the cavities and pores of this adsorbent.

3.3. Effect of adsorbate concentrations

The removal of azorhodanine dye (AR) by adsorption on the adsorbent (RSFA) was shown to increase with time and attained a maximum value at about 75 min, and thereafter, it remained almost constant (Fig. 2). On changing the initial concentration of dye solution from 20 to 100 mg/L at 25 ºC, pH 3 and 0.07 g/L adsorbent dosage the amount of removed dyes was decreased. It was clear that the removal of the dye was dependent on the initial concentration of the dye because the decrease in the initial dye concentration increased the amount of dye adsorbed. This is very clear because, for a fixed adsorbent dose, the number of active adsorption sites to

accommodate adsorbate ions remains unchanged but with increasing adsorbate concentration, the adsorbate ions to be accommodated increase and hence the percentage of adsorption goes down.
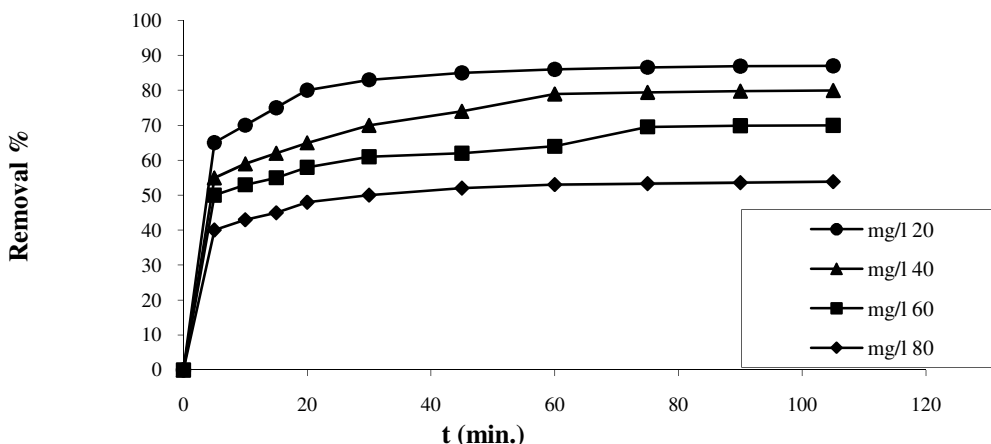
Fig. 2. Effect of intial dye concentration on
adsorption of AR onto RSFA, dosage 0.07 g/l, pH = 3 and 25 ºC.

3.4. Effect of adsorbent dosage

The uptake of dye with change in adsorbent dosage (0.05–0.8 g) at adsorbate concentrations of 100 mg/L at 25 ºC and pH 3 is presented at (Fig. 3). Adsorption of dye shows that the uptake of dye per gram of adsorbent increases with increasing adsorbent dosage from 0.05 to 0.8 g. This is because a higher dose of adsorbent, led to increased surface area and more adsorption sites are available causing higher removal of the dye. Further increase in adsorbent dose, did not cause any significant increase in % removal of dye. This was due to the concentration of dyes reaching equilibrium status between solid and solution phase.
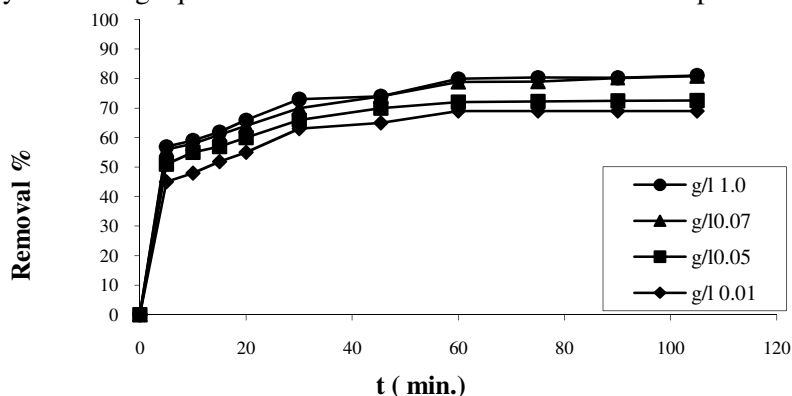
Fig. 3. Effect of RSFA dosage on the adsorption
of AR at concentration 100 mg/l, pH=3 and 25 ºC .

3.5. Effect of temperature

The results of this study are shown (Fig. 4) which explain the relation between the removal of dye ratio and time at different temperatures (25, 40, 50 and 60ºC) using the (RSFA) adsorbent reveal that the contact time decrease with increasing temperature this might be due to increasing diffusion coefficient with the increase in temperature. In our case the experimental data obtained at pH 3, adsorbent dosage 0.07 g/L, and initial concentration of 100 mg/L show that increase in the adsorption capacity at temperatures from 25 to 60 ºC.
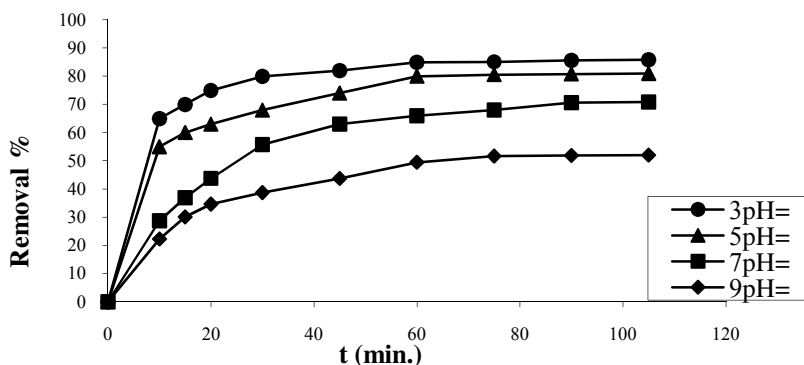
3.6. Effect of pH

The removal of the tested dye by activated carbon of rice straw (RSFA) at different pH values was studied at initial concentrations of 100 mg/L of the dye, 25 ºC and 0.07 g/L adsorbent dosage. The pH value of the solution was an important controlling parameter in the adsorption process. RSFA has proved to be an effective

adsorbent for the removal of the dye, which was achieved via adsorption from an aqueous solution at pH 3 was achieved (Fig. 5). It shows that the adsorption capacity of tested dye onto RSFA increases significantly with decreasing pH. The maximum removals for contact time 75 min.were carried out at pH 3.
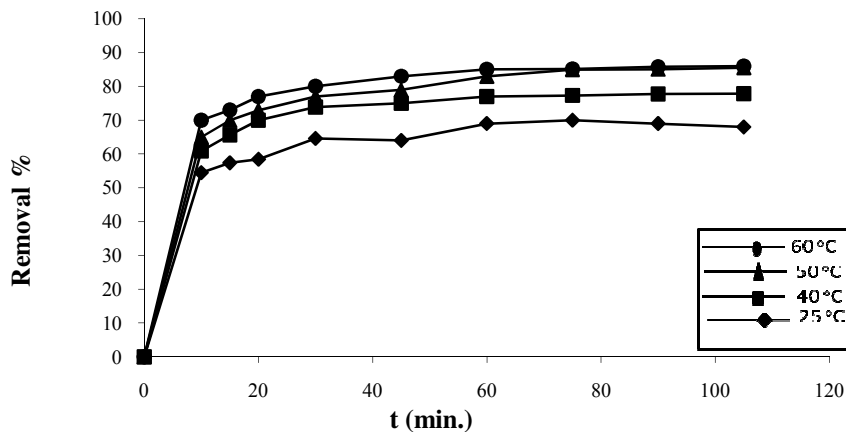
Fig. 4.   Effect of temperature on the adsorption of AR onto RSFA, weight
of adsorbent 0.07 g/l, dye concentration 100 mg/l and pH=3.

As the pH of the adsorption system increases, the number of negatively charged sites increases and the number of positively charged sites decreases. A negatively charged surface site on the adsorbent does not favor the adsorption of dye anions, due to the electrostatic repulsion. Also, lower adsorption of tested dye at alkaline pH is due to the presence of excess hydroxyl ions competing with the dye anions for the adsorption sites [31,32].

Fig. 5 . Effect of pH on adsorption of AR onto RSFA,
weight of adsorbent 0.07 g/l and temperature 25 °C.

3.7. Adsorption Isotherms
The main factors that play the key role for the dye-adsorbent interactions are charge and structure of dye, adsorbent surface properties, hydrophobic and hydrophilic nature, hydrogen bonding, electrostatic interaction, steric effect, and van der Waal forces etc. [33]. Equilibrium studies that give the capacity of the adsorbent and adsorbate are described by adsorption isotherms, which is usually the ratio between the quantity adsorbed and that remained in solution at equilibrium at fixed temperature [34–36]. The equilibrium experimental data for the adsorption of the tested dye on the (RSFA) was compared using two isotherm equations namely, Langmuir and Freundlich.

3.7.1. Langmuir isotherm
The Langmuir adsorption, which is the monolayer adsorption, depends on the assumption that the intermolecular forces decrease rapidly with distance and consequently predicts the existence of monolayer coverage of the adsorbate at the outer surface of the adsorbent. The isotherm equation further assumes that

adsorption occurs at specific homogeneous sites within the adsorbent. It then assumed that once a dye molecule occupies a site, no further adsorption can take place at that site. Furthermore, the Langmuir equation is based on the assumption of a structurally homogeneous adsorbent, where all sorption sites are identical and energetically equivalent. Theoretically, the sorbent has a finite capacity for the sorbate. Therefore, a saturation value is reached beyond which no further sorption can occur. The saturated or monolayer capacity can be represented as the known linear form of Langmuir equation [37-41],

$C_e / q_e = 1/ (q_{max} K_L) + C_e / q_{max}$ (4)

where C_e is the equilibrium dye concentration in the solution (mg/L), q_e is the equilibrium dye concentration in the adsorbent (mg/g), q_{max} is the monolayer capacity of the adsorbent (mg/g) and K_L is the Langmuir adsorption constant (L/mg).

Therefore, a plot of C_e/q_e *vs.* C_e (Fig.6), gives a straight line of slope $1/q_{max}$ and the intercept $1/(q_{max} K_L)$. The Langmuir equation is applicable to homogeneous sorption, where the sorption of each sorbate molecule onto the surface is equal to the sorption activation energy.
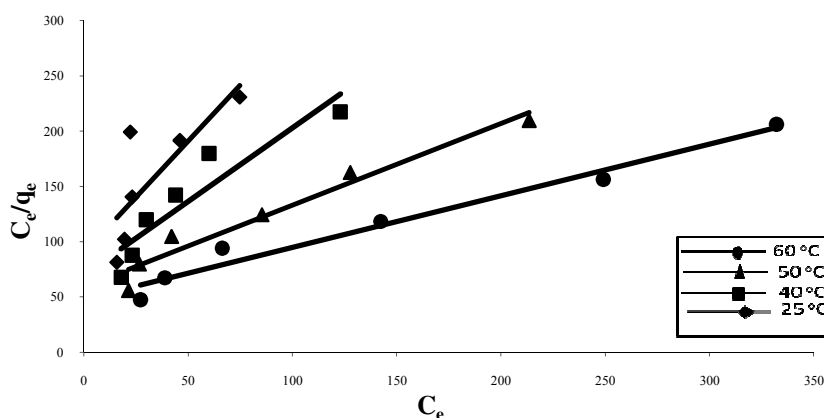

Fig. 6. Langmuir plot for the adsorption of AR onto RSFA at different temperatures.

3.7.2. Freundlich isotherm

The Freundlich equation [40-42] is an empirical equation employed to describe heterogeneous systems, characterized by the heterogeneity factor 1/n, describes reversible adsorption and is not restricted to the formation of the monolayer:

$q_e = K_F . C_e^{1/n}$ (5)

where q_e is the equilibrium dye concentration on adsorbent (mg/g), C_e is the equilibrium dye concentration in solution (mg/L), K_F is Freundlich constant (L/g) and 1/n is the heterogeneity factor. A linear form of the Freundlich expression can be obtained by taking logarithms of the equation

$\log q_e = \log K_F + 1/n . \log C_e$ (6)

Therefore, a plot of log q_e *vs.* log C_e for the adsorption of tested dye onto RSFA (Fig. 7) was employed to generate the intercept value of K_F and the slope of 1/n. The correlation coefficients for Langmuir (r_L^2) and for Freundlich (r_F^2) values are compared in Table 1.

Table 1. Langmuir and Freundlich parameters for the adsorption of AR onto RSFA.

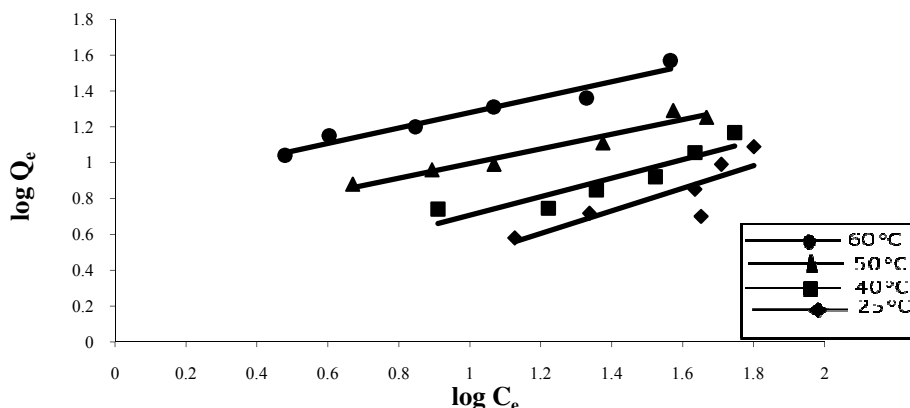| Temperature (°C)	Langmuir isotherm			Freundlich isotherm		
	q_{max} (mg/g)	K_L (L/mg)	r_L^2	K_F (mg/g)	n	r_F^2
25	69.78	0.0106	0.827	1.342	1.891	0.981
40	94.6671	0.0231	0.878	1.618	1.632	0.986
50	129.56	0.0272	0.892	1.882	1.489	0.994
60	148.584	0.0315	0.904	2.204	1.304	0.999

Fig. 7. Freundlisch plots for the adsorption of AR onto RSFA at
different temperatures.

One of the Freundlich constants K_F indicates the adsorption capacity of the adsorbent. The other Freundlich constant n is a measure of the deviation from linearity of the adsorption. If a value for n is equal to unity the adsorption is linear. If a value for n is below to unity, this implies that the adsorption process is chemical, but a value for n is above to unity, adsorption is favorable a physical process [43]. The highest value of n at equilibrium is 1.891 (Table 1), which would seem to suggest that the adsorption is physical, which is referred the adsorption bond which becomes weak [44] and conducted with van der Waals forces.

3.8. Adsorption kinetic studies

The study of adsorption kinetics describes the solute uptake rate and evidently this rate controls the residence time of adsorbate uptake at the solid-solution interface. The rate of removal of tested dye by adsorption was rapid initially and then slowed gradually until it attained an equilibrium beyond which there was a significant increase in the rate of removal. The maximum adsorption was observed at 75 min. and it is thus fixed as the equilibrium time. Aiming at evaluating the adsorption kinetics of tested dye onto (RSFA), the pseudo-first-order and pseudo-second-order kinetic models were used to fit the experimental data, according to the below kinetic model equations.

The pseudo-first-order rate expression of Lagergren [45,46] is given as:

$$\log (q_e - q_t) = \log q_e - k_1 t \qquad (7)$$

The pseudo-second-order kinetic model [45] is expressed as:

$$t/q_t = 1/k_2 q_2^2 + 1/q_2\, t \qquad (8)$$

where *qt* is the amount of dye adsorbed (mg/g) at various times *t*, q_e is the maximum adsorption capacity (mg/g) for pseudo-first-order adsorption, k_1 is the pseudo-first-order rate constant for the adsorption process (min^{-1}), q_2 is the maximum adsorption capacity (mg/g) for the pseudo-second-order adsorption, k_2 is the rate constant of pseudo-second-order adsorption ($g\,mg^{-1}\,min^{-1}$). The straight-line plots of $\log (q_e - qt)$ versus *t* for the pseudo-first-order reaction and *t/qtvs.t* for the pseudo-second-order reaction (Figs. 8 and 9) for the adsorption of tested dye onto (RSFA) have also been tested to obtain the rate parameters. The k_1, k_2, q_e, q_2, and correlation coefficients, r_1^2 and r_2^2 for the dye under different temperatures were calculated from these plots and are given in Table 2.

Table 2. Pseudo-first-order and Pseudo-second-order for the adsorption of AR onto RSFA.

Temperature (^oC)	Pseudo-first-order			Pseudo-second-order		
	q_e (mg/g)	k_1 (min^{-1})	r_1^2	q_2 (mg/g)	k_2 ($g\,mg^{-1}\,min^{-1}$)	r_2^2
25	0.903	3.69	0.899	161.04	0.169	0.987
40	0.914	3.49	0.993	160.97	0.214	0.998
50	0.922	2.98	0.994	160.01	0.479	0.998
60	0.938	2.32	0.996	160.09	0.589	0.998

The correlation coefficients (r_1^2) for the pseudo-first-order kinetic model are between 0.899 and 0.996 and the correlation coefficients (r_2^2), for the pseudo-second-order kinetic model are between 0.987 and 0.998. It is probable, therefore, that this adsorption system is not a pseudo-first-order reaction, as it fits the pseudo-second-order kinetic model.
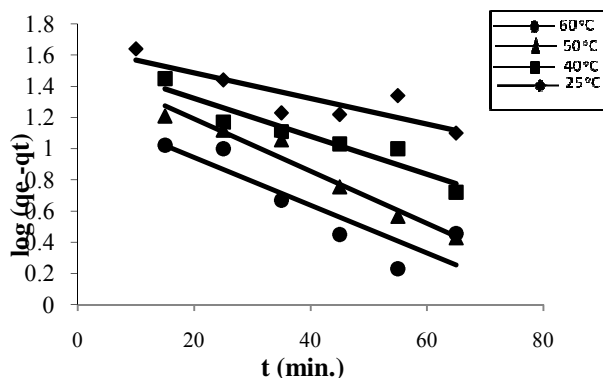
Fig. 8. Pseudo-first-order kinetic plot for the adsorption of AR onto RSFA at different temperatures.
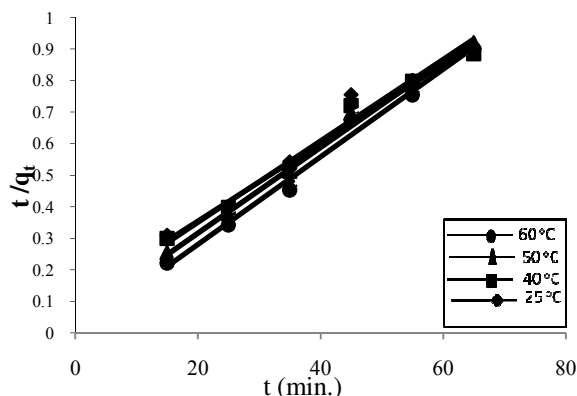

Fig. 9. Pseudo-second-order kinetic plot for the adsorption of AR onto RSFA at different temperatures.

3.9. Thermodynamic parameters

In any adsorption process, both energy and entropy considerations must be taken into account in order to determine what process will occur spontaneously. Values of thermodynamic parameters are the actual indicators for practical application of a process. The amount of the dye adsorbed onto (RSFA) at equilibrium and at different temperatures 25, 40, 50, 60 ^{o}C, has been examined to obtain thermodynamic parameters for the adsorption system. The pseudo-second-order rate constant of tested dye adsorption is expressed as a function of temperature by the following Arrhenius type relationship [47]:

$$\ln k_2 = \ln A - E_a/RT \qquad (9)$$

where E_a is the Arrhenius activation energy of adsorption, A is the Arrhenius factor, R is the gas constant and is equal to 8.314 J.mol^{-1} K^{-1} and T is the operated temperature. A linear plot of $\ln k_2$ *vs.* 1/T for the adsorption (Fig. 10) was constructed to generate the activation energy from the slope ($-E_a/R$).
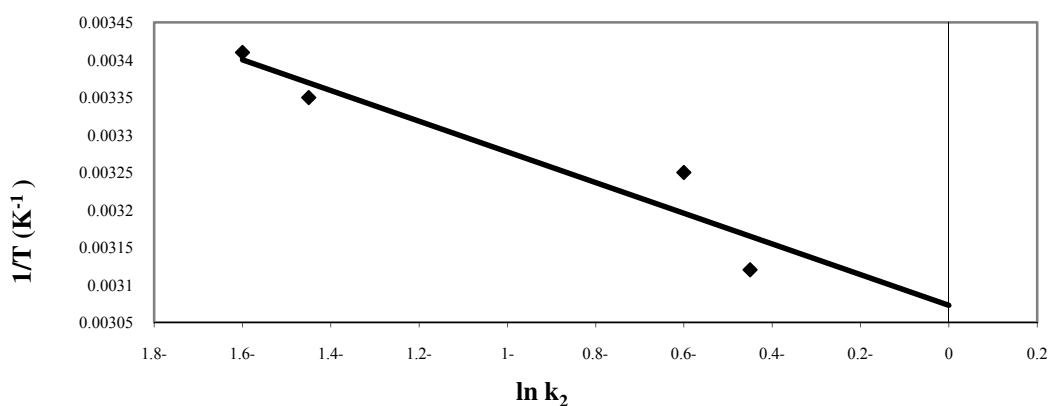
Fig. 10. Arrhenius plot of the adsorption of AR onto RSFA.

The chemical (chemisorption) or physical (physisorption) adsorption mechanism are often an important indicator to describe the type of interactions between tested dye and (RSFA). The magnitude of activation energy gives an idea about the type of adsorption which is mainly physical or chemical. Low activation energies (5–40 kJ mol^{-1}) are characteristics for physisorption, while higher activation energies (40–800 kJ mol^{-1}) suggest chemisorption [48]. The result obtained is +11.09 kJ mol^{-1} (Table 3) for the adsorption of the dye onto (RSFA), indicating that the adsorption has a low potential barrier and corresponding to a physisorption.

Table 3. Thermodynamic parameters calculated with the pseudo-second rate constant for the adsorption of AR onto RSFA.

| Temperature (^{o}C)	K_c	E_a (kJ mol^{-1})	ΔG^o (kJ mol^{-1})	ΔH^o (kJ mol^{-1})	ΔS^o (J.mol^{-1}.K^{-1})
25	96.64		-34.167		
40	123.07	11.09	-34.525	-10.38	0.097
50	234.33		-34.856		
60	203.30		-35.065		

The other thermodynamic parameters, change in the standard free energy (ΔG^o), enthalpy (ΔH^o) and entropy (ΔS^o) were determined by using following equations:

$$K_C = C_A/C_S \qquad (10)$$
$$\Delta G^o = -RT \ln K_C \qquad (11)$$
$$\ln K_C = \Delta S^o/R - \Delta H^o/RT \qquad (12)$$

where K_C is the equilibrium constant, C_A is the amount of dye adsorbed on the (RSFA) of the solution at equilibrium (mol L^{-1}), and C_S is the equilibrium concentration of the dye in the solution (mol L^{-1}). The q_2 of the pseudo-second-order model in Table 3 was used to obtain C_A and C_S. T is the solution temperature (K) and R is the gas constant. ΔH^o and ΔS^o were calculated from the slope and the intercept of Van't Hoff plots of ln K_C *vs.* 1/T (Fig. 11). The results are given in Table 3.
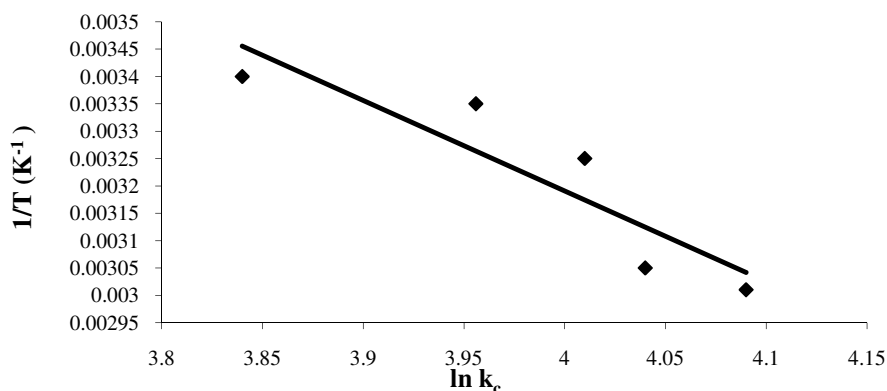
Fig. 11. Van't Hoff plot for determination of thermodynamic parametets for the adsorption of AR onto RSFA.

The values of adsorption thermodynamic parameters are listed in Table 3. The negative value of the change of free energy (ΔG^o) confirms the feasibility of the adsorption process and also indicates spontaneous adsorption of tested dye onto (RSFA) in the temperature range studied [49]. The small negative value of the standard enthalpy change (ΔH^o) which is (-10.38 kJ mol^{-1}) indicates that the adsorption is physical in nature involving weak forces of attraction and is also exothermic, thereby demonstrating that the process is stable energetically. The low positive value of ΔS^o (0.097J.mol^{-1}K^{-1}) suggest that the increased randomness of the solid-solution interface during the adsorption of AR in aqueous solution on ACRS [50].

Conclusion

From the present study which clearly demonstrated that activated carbon made from rice straw(RSFA) are an effective adsorbent for the removal of azorhodanine from an aqueous solution and polluted water. The high adsorption capacity of azorhodanineonto RSFA in highly acidic solutions (pH 3) is due to the strong electrostatic interactions between its adsorption site and dye anion. The Brunauer-Emmett-Teller (BET) surface area and Barrett-Joyner-Halenda (BJH) pore volume were calculated and found to be 67.4 m^{2}g^{-1}and 0.134 cm^{3}g^{-1}, respectively. SEM images shows well defined and characterized morphological images that are evident for the effective adsorption of azorhodanine molecules on the cavities and pores of the (RSFA). For the application of Langmuir and Freundlich equations, the experimental results shows that the Freundlich model was the best. The highest value of n at equilibrium is 1.751suggest that the adsorption is physical. The kinetic data tends to fit very well in the pseudo-second-order kinetics model with high correlation coefficients. The ΔG^o values were negative; therefore the adsorption was spontaneous in nature. The negative value of ΔH^o reveals that the adsorption process was exothermic in nature and a physical adsorption. The positive value of ΔS^o implies that the increment of an orderliness between the adsorbate and the adsorbent molecules. Finally, the adsorbent RSFA displayed the main advantages of excellent dispersion in an aqueous solution, separation convenience and high adsorption capacity, which implied their application potentials for effective removal of other hazardous pollutants from an aqueous solution.

References

1. Kalburc T., Tabak A., Ozturk N., Tuzmen N., Akgol S., Caglar B., Denizli A., *J. Mol. Struct.* 1083 (2015) 156.
2. Melo R.P.F., Barros Neto E.L., Moura M.C.P.A., Castro Dantas T.N., DantasNeto A.A., Oliveira H.N.M., *Sep. Purif. Technol.* 138 (2014) 71.
3. Ma T.T., Chang P.R., Zheng P.W., Zhao F., Ma X.F., *Chem. Eng. J.* 240 (2014) 595.
4. Patil M.R., Shrivastava V.S., *J. Mater. Environ. Sci.* 6(1) (2015) 11.
5. Ghaedi M., Khajehsharifi H., HemmatiYadkuri A., Roosta M., Asghari A., *Toxicol. Environ. Chem.* 94 (2012) 873.
6. Ammar T.A., Abid K.Y., El-Bindary A.A., El-Sonbati A.Z., *Desalination* 352 (2014) 45.
7. El-Bindary A.A., Hussien M.A., Diab M.A., Eessa A.M., *J. Mol. Liq.* 197 (2014) 236.
8. El-Bindary A.A., Diab M.A., Hussien M.A., El-Sonbati A.Z., Eessa A.M., *Spectrochim. Acta A* 124 (2014) 70.
9. Ghaedi M., Ansari A., Habibi M.H., Asghari A.R., *J. Ind. Eng. Chem.* 20 (2014) 17.
10. Fathi M.R., Asfaram A., Farhangi A., *Spectrochim. Acta A* 135 (2015) 364.
11. Ghaedi M., Ghaedi A.M., Ansari A., Mohammadi F., Vafaei A., *Spectrochim. Acta A* 132 (2014) 639.
12. Sajab M.S., Chia C.H., Zakaria S., Khiew P.S., *Bioresour. Technol.* 128 (2013) 571.
13. Wang S.B., Boyjoo Y., Choueib A., Zhu Z.H., *Water Res.* 39 (2005) 129.
14. Faria P.C.C., Orfao J.J.M., Pereira M.F.R., *Water Res.* 38 (2014) 2043.
15. El-Bindary A.A., El-Sonbati A.Z., Al-Sarawy A.A., Mohamed K.S., Farid M.A., *J. Mol. Liq.* 199 (2014) 71.
16. Roosta M., Ghaedi M., Shokri N., Daneshfar A., Sahraei R., Asghari A., *Spectrochim. Acta A* 118 (2014) 55.
17. Madaeni S.S., Jamali Z., Islami N., *Sep. Purif. Technol.* 81 (2011) 116.
18. Serpone N., Horikoshi S., Emeline A.V., *J. Photochem. Photobiol. C* 11 (2010) 114.
19. Kyzas G.Z., Deliyanni E.A., Lazaridis N.K., *J. Coll. Interf. Sci.* 430 (2014) 166.
20. Asgher M., Bhatti H.N., *Ecological Eng.* 38 (2012) 79.
21. Yang S., Gao M., Luo Z., *Chem. Eng. J.* 256 (2014) 39.
22. El-Bindary A.A., El-Sonbati A.Z., Al-Sarawy A.A., Mohamed K.S., Farid M.A., *Spectrochim. Acta A* 136 (2015) 1842
23. Visa M., Duta A., *J. Hazard. Mater.* 244 (2013) 773.
24. Wang S., Zhu Z.H., *J. Hazard. Mater. B* 126 (2005) 91.
25. Wang S., Boyjoo Y., Choueib A., *Chemosphere* 60 (2005) 1401.
26. Gupta V.K., Mohan D., Sharma S., Sharma M., *Sep. Sci. Technol.* 35 (2000) 2097.
27. El-Sonbati A.Z., El-Bindary A.A., Abd El-Mksoud S.A., Belal A.A.M., El-Boz R.A., *J. Mol. Liq.* 199 (2015) 538.
28. Daffalla S.B., Mukhtar H., Shaharun M.S., *J. Appl. Sci.* 10 (2010) 1060.
29. Foo K.Y., Hameed B.H., *Chem. Eng. J.* 156 (2010) 2.
30. Brunauer S., Emmett P.H., Teller E., *J. Am. Chem. Soc.* 60 (2002) 309.
31. Alkan M., Demirbas O., Celikcapa S., Dogan M., *J. Hazard. Mater.* 116 (2004) 135.
32. Khan M.R., Ray M., Guha A.K., *Bioresour. Technol.* 102 (2011) 2394.
33. Ahmad R., Kumar R., *J. Environ. Mang.* 91 (2010) 1032.
34. Guendy H.R.,*J. Appl. Sci. Res.* 6(8) (2010) 964.
35. Kiran I., Akar T., Ozcan A.S., Ozcan A., Tunali S.,*Biochem. Eng. J.* 31 (2006) 197.
36. Yavuz M., Gode F., Pehlivan E., Ozmert S., Sharma Y.C., *Chem. Eng. J.* 137 (2008) 453.
37. Langmuir I., *J. Am. Chem. Soc.* 38 (1916) 31.
38. Langmuir I., *J. Am. Chem. Soc.* 39 (1917) 1848.
39. Langmuir I., *J. Am. Chem. Soc.* 40 (1918) 1361.
40. Alley A.R., "Water quality control handbook", *McGraw-Hill Education*: Europe: London, (2000).
41. Woodard F., "Industrial waste treatment handbook", *Butterworth-Heinemann*: Boston, (2001).
42. Freundlich H.M.F., *Z. Phys. Chem. (Leipzig)* 57A (1906) 385.
43. Tunali S., Ozcan A.S., Ozcan A., Gedikbey T., *J. Hazard. Mater.* B135 (2006) 141.
44. Jiang J.-O., Cooper C., Ouki S., *Chemosphere* 47 (2002) 711.
45. Lagergren S., *Handlingar* 24 (1898) 1.
46. Ho Y.S., McKay G., *Chem. Eng. J.* 70(2) (1998) 115.
47. Juang R.S., Wu F.C., Tseng R.L., *Environ. Technol.* 18(5) (1997) 525.
48. Nollet H., Roels M., Lutgen P., Van der Meeren P., Verstraete W., *Chemosphere* 53(6) (2003) 655.
49. Jaycock M.J., Parfitt G.D., "Chemistry of Interfaces", *Ellis Horwood Ltd*, Onichester, (1981).
50. El-Bindary A.A., El-Sonbati A.Z., Al-Sarawy A.A., Mohamed K.S., Farid M.A., *J. Mater. Environ. Sci.* 6 (2015) 1.